

Version submitted to ApJL on December 3 2002

***XMM-Newton* detection of warm/hot intergalactic medium at $z \sim 0.01$**

I. Cagnoni¹

Dipartimento di Scienze, Università dell'Insubria Via Valleggio 11, I-22100, Como, Italy

ABSTRACT

We report a $\simeq 3\sigma$ detection of a 21.82 Å absorption feature in the direction of the BL Lac MRK 421 which is interpreted as O VII K α at $z \simeq 0.01$. This corresponds to the redshift of a H absorber in a cosmic void detected by HST along the line of sight of the same object. The 21.82 Å line proves the existence of warm/hot intergalactic medium (WHIM) outside the Local Group, in agreement with current models of structure formation in the Universe. The WHIM at $z \sim 0.01$ has temperature of $\lesssim (2.5 - 4) \times 10^6$ K for gas densities in the range $10^{-6} - 1$ atom cm⁻³. We also detect O VII, O VIII and Ne IX absorption lines with zero velocity, possibly connected with WHIM in the Local Group.

Subject headings: BL Lacertae objects: individual (MRK 421) — intergalactic medium — large-scale structure of universe — quasars: absorption lines

1. Introduction

In the local Universe $\sim 50 - 60\%$ of the baryons visible at $z > 2$ and predicted by the Standard Big-Bang nucleosynthesis are undetected (e.g. Fukugita, Hogan, & Peebles 1998). Numerical simulations predict that such baryons, in the form of Ly α clouds (i.e. gas at $T < 10^4$ K) and visible in the UV spectra of bright AGNs, have been shock-heated during the formation of the structures in the Universe to temperatures of $\sim 10^5 - 10^7$ K (i.e. the warm hot intergalactic medium, WHIM). The most efficient way to detect such gas is through resonant absorption lines from highly ionized metals (e.g. OVI, OVII, OVIII, NeIX) in the far UV and soft X-ray spectra of background sources (e.g. Hellsten, Gnedin, & Miralda-Escudé 1998; Fang & Canizares 2000). Current far UV observations proved the existence of the low temperature tail ($T \sim (1 - 5) \times 10^5$ K) of the WHIM through the detection of OVI up to $z \sim 0.2$ (e.g. Sembach et al. 2000; Tripp et al. 2001). However the bulk of the

WHIM baryons ($\sim 70\%$, e.g. Fukugita, Hogan, & Peebles 1998) are expected to lie at higher temperatures ($T \sim 10^6 - 10^7$ K) and their features should be detectable in the soft X-ray regime. *Chandra* and *XMM-Newton* high resolution spectroscopy ($R \sim 100 - 500$) brought to the detection of a “zero redshift” OVII absorption feature at 21.6 \AA in the spectra of four bright AGNs (PKS 2155-304, Nicastro et al. 2002; Fang et al. 2002; Cagnoni et al. 2003; 3C 273, Fang, Sembach & Canizares 2003; H1821+643, Mathur, Weimberg & Chen 2002 and MRK 421, Nicastro et al. 2001), interpreted as the signature of WHIM present within the Local Group. The only published evidence of WHIM outside the Local Group is at $z \sim 0.05$ (Fang et al. 2002), however this feature is not confirmed in other *Chandra* and *XMM-Newton* observations (e.g. Nicastro et al. 2002; Cagnoni et al. 2003). In this paper I present strong evidence for an OVII $K\alpha$ absorption line at $z \sim 0.01$ in the spectrum of the BL Lac object MRK 421.

The paper is organized as follows: § 2 reports the *XMM-Newton* observations of MRK 421 and describes the data reduction; § 3 contains the spectral fits and the discussion on the observed WHIM absorption features. § 4 is a conclusive section containing a summary of the results.

2. Observations and data reduction

MRK 421 is a calibration target for *XMM-Newton* and has been observed several times from the launch (Dec. 10, 1999) up to the time of writing. Table 1 summarizes all the public observations as of December 3, 2002. MRK 421 X-ray spectrum is thought to be relativistically beamed synchrotron emission from energetic electrons and its intrinsic lack of features is the ideal laboratory to search for faint WHIM absorption lines. In this paper I will concentrate on the high resolution ($\Delta E/E$ from 100 to 500, FWHM, or 100 to 800, HEW, in the energy range 0.33–2.5 keV - 5–38 \AA) Reflection Grating Spectrometers (RGS1 and RGS2) data collected by the two *XMM-Newton* X-ray telescopes¹. *XMM-Newton* RGS effective areas are complex in shape, and contain tens of narrow dips due to bad or hot columns or pixels in the CCD detectors, which require extremely accurate calibration measurements for a proper modeling (e.g. Cagnoni et al. 2003). Current RGS calibration uncertainties are as accurate as $\sim 5 - 10\%$ between 7 and 36 \AA and, as a consequence, false absorption/emission features with such relative intensities, are expected in the RGS spectra in physical units, in proximity of the known instrumental features. The strongest resonant absorption lines from neutral and/or highly ionized O and Ne, fall in wavelength ranges (i.e. 13-14 \AA , 18-20

¹I refer the reader to Sembay et al. (2002) for a detailed description of the observations and for and accurate spectral and timing analysis of EPIC data collected in 2000 and 2001.

Å, 20-24 Å) in which RGS-2 spectra either do not exist (20-24 Å, due to the failure of a CCD chip) or contain strong line-like shaped instrumental features (see Cagnoni et al. 2003). Therefore I rely on RGS-1 spectra, which, instead are relatively instrumental-feature-free in these wavelength ranges, and use RGS-2 to double check the reality of a line, when possible, and to cover the 10.5-14.2 Å region, where RGS-1 has a failed CCD chip. I also restrict our analysis to the first order spectra only.

I reprocessed the data using *XMM-Newton Science Analysis System* (SAS) version 5.3.0 and the latest calibration files as of December 3, 2002. Since the wavelength calibration of XMM grating spectra strongly depends on the position of the 0th order, I used the VLBI position as centroid of the 0th order source (Ma et al. 1998). Extraction regions, for source and background, were chosen to be, respectively, within the 95% and outside the 98% of the PSF. To exclude high particle background periods caused by solar activity, I extracted the background lightcurves from CCD-9 and excluded all the time intervals for which the background count rate was higher than 1.5×10^{-3} count s⁻¹. The net exposures for each observation are reported in Table 1.

In order to improve the signal to noise ratio (SNR) I combined all the RGS-1 order 1 spectra obtained with a pointing offset $< 15''$ ² (see Table 1) and computed the combined RGS-1 response matrixes (a convolution of the detector response matrix and effective area, Fig. 1) using the PINTofALE interactive data language software suite (Kashyap & Drake 2000). I did the same for RGS-2. The total net exposures are 125 ks and 122 ks for RGS-1 and RGS-2 respectively.

3. The WHIM detection

I fit the combined fluxed RGS-1 spectrum in the wavelength range 14.2–38.1 Å using version 2.2 of SHERPA (Siemiginowska et al., in prep.) modeling and fitting tool from the CXC analysis package CIAO 2.2 (Elvis et al., in prep.). I used an absorbed power law model with absorption characterized by a column density $N(X)$ and an absorption cross section σ_X for each element. I included in the model H, He I and He II (Rumph, Bowyer, & Vennes 1994) and heavier elements (Morrison & McCammon 1983). I fixed the Galactic

²The inclusion of the off-axis data in the combined spectrum increases the number of photons at 20 Å from ~ 4000 to ~ 7000 per 0.06 Å resolution element, but degrades the quality of the spectrum. May 2002 observations, for example, are highly affected by hot columns and pixels which result in spurious features in and around the expected WHIM lines. To reduce the impact of hot columns and pixels, the RGS units have recently been cooled (November 2002).

hydrogen column density at $N_H = 1.61 \times 10^{20} \text{ cm}^{-2}$ (Lockman & Savage 1995) and the ratios $N_{\text{HeI}}/N_{\text{HI}}=0.1$ and $N_{\text{HeII}}/N_{\text{HI}}=0.01$. The best fit RGS-1 photon slope is $\Gamma_\lambda = 0.095 \pm 0.004$ (corresponding to an energy photon slope of 2.095 ± 0.004) and the normalization is $0.0136 \text{ photons cm}^{-2} \text{ s}^{-1} \text{ \AA}^{-1}$ at 20.5 \AA . In order to properly model the continuum around the expected WHIM features, I performed local absorbed power-law fits in the $18.0\text{--}20.6 \text{ \AA}$ and in the $20.9\text{--}22.4 \text{ \AA}$ regions. I kept the absorbing column fixed to the Galactic value in MRK 421 direction and modeled the absorption lines with Gaussian. The lines detected at $> 2\sigma$ and the corresponding best fit parameters are listed in Table 2.

It appears to us that the only possible interpretation of the 21.82 \AA line (2.8σ detection; Fig. 1) is redshifted O VII K α . This places the gas producing it at $z \sim 0.01$ and makes this a solid X-ray detection of WHIM outside our local group of Galaxies. The corresponding $z \sim 0.01$ O VII K β is expected to be too faint ($\text{EW} \sim 0.8 \text{ m\AA}$ at $\sim 18.84 \text{ \AA}$) to be detected in this spectrum. If any O VIII were present in the $z \sim 0.01$ WHIM, the strongest expected line would be Ly α at 19.18 \AA , not detected in our spectrum. The 3σ upper limit on the line EW, computed fixing the line FWHM to the 21.82 \AA line FWHM value, is 2.47 m\AA . Under the assumption of unsaturated line the EW ratios between different species depend on the gas temperature and density. Using the ratio between the upper limit on the EW of O VIII at $z \sim 0.01$ and the 21.82 \AA line EW, I obtain an upper limit on the $z \sim 0.01$ gas temperature of $\sim 4 \times 10^6 \text{ K}$, for a gas density of 1 atom cm^{-3} and of $\sim 2.5 \times 10^6 \text{ K}$, for a gas density of $10^{-6} \text{ atom cm}^{-3}$ (see Fig. 5 in Nicastro et al. 2002). These values are consistent with the temperature range predicted for the WHIM emitting in the soft X-ray band. I derive from the 21.82 \AA line a velocity of $cz \sim 3062 \text{ km s}^{-1}$, consistent, within the errors, with the redshift of a strong H Ly α line detected by HST on MRK 421 spectrum ($cz = 3035 \pm 6 \text{ km s}^{-1}$) and coming from absorbing material in a cosmic void (Shull, Stocke, & Penton 1996; Penton, Stocke, & Shull 2000). The location of WHIM in a cosmic void is consistent with the picture that such gas is connecting the overdense regions of the sky that collapsed into clusters and groups during the structures formation.

For the other lines listed in Table 2, the strongest is the O VII K α absorption at 21.6 \AA (Fig. 1); the corresponding O VII K β is visible at 18.67 \AA (Fig. 2). The 21.6 \AA feature has already been seen in MRK 421 itself (Nicastro et al. 2001) and in other 4 AGNs (Nicastro et al. 2002; Fang et al. 2002; Cagnoni et al. 2003; Mathur, Weimberg & Chen 2002; Fang, Sembach & Canizares 2003) and it is usually attributed to a WHIM within our local group of galaxies (e.g. Nicastro et al. 2002) or to radiatively cooling gas inside our Galaxy (e.g. Heckman et al. 2002). I also report the detection of zero redshift O VIII Ly α at 18.97 \AA (Fig. 2) and of NeIX K α at 13.4 \AA (Fig. 3). Note however that these lines are affected by small features in the effective area.

The EW of the zero redshift features (O VII, O VIII and NeIX) are compatible with those measured with *Chandra* for PKS2155-304 (Nicastro et al. 2002; Fang et al. 2002) and for

MRK 421 (Nicastrro et al. 2001). In particular, the EW derived fixing the lines FWHM to the value of the 21.6 Å line, (i.e. 0.33, 0.27 and 0.20 eV respectively) are consistent with the lines being unsaturated and with column densities of $\sim 10^{16}$ atoms cm^{-2} per ion species (see Fig. 4 in Nicastrro et al. 2002). For a gas density of $\sim 10^{-6}$ atoms cm^{-3} , NeIX/OVII and O VIII/OVII ratios indicate gas temperatures of $\sim (0.4 - 2) \times 10^6$ K, and $\sim (1 - 4)10^6$ K, respectively (Fig. 5 of Nicastrro et al. 2002). These ranges move to $\sim (1.5 - 2.5) \times 10^6$ K and $\sim (3 - 4) \times 10^6$ K in case of Galactic gas density. Even if these estimates have to be regarded with caution because of the possible modifications of the effective area features, they are all consistent with the range of temperatures predicted for the WHIM.

4. Conclusion

I report strong evidence of WHIM outside our local group of galaxies through the detection of a 21.82 Å O VII K α absorption line in the *XMM-Newton* RGS-1 spectrum of MRK 421. The line redshift is ~ 0.01 , in agreement with that derived for the strong H Ly α absorption line detected by HST and related to an absorber in a cosmic void. The three closest galaxies are at 2.14, 3.98 and 4.12 h_{70}^{-1} Mpc (Penton, Stocke, & Shull 2000). This detection is a firm proof the existence of a WHIM filament at $z \sim 0.01$ possibly connecting the nearby galaxies with other denser regions of the sky, as expected by the models of the cosmic structures formation and evolution. I derive an upper limit on the gas temperature of $\sim 2.5 - 4 \times 10^6$ K for a gas density of $10^{-6} - 1$ atom cm^{-3} . The only known similar evidences are a 4.5σ detection of O VIII at $z \sim 0.05$ reported by Fang et al. (2002) in the *Chandra* spectrum of PKS 2155-304 and the $\sim 2\sigma$ detections of two O VII lines at $z \sim 0.2$ in the *Chandra* spectrum of H1821+643 (Mathur, Weimberg & Chen 2002). However Fang et al. (2002) feature is not confirmed in other *Chandra* and *XMM-Newton* observations (e.g. Nicastrro et al. 2002; Cagnoni et al. 2003).

I also detect the zero redshift absorption features of O VII, OVII and NeIX with positions and EWs consistent with previous detections in the direction of other bright AGNs (e.g. Nicastrro et al. 2002; Cagnoni et al. 2003).

I acknowledge a C.N.A.A. fellowship. I thank Aldo Treves and Francesco Haardt for useful scientific discussions and a careful reading of the manuscript.

REFERENCES

- Cagnoni, I. et al., 2003, ApJ in preparation
- Fang, T. & Canizares, C. R. 2000, ApJ, 539, 532
- Fang, T., Marshall, H. L., Lee, J. C., Davis, D. S., & Canizares, C. R. 2002, ApJ, 572, L127
- Fang, T. , Sembach, K. R. & Canizares, C. R., 2003, ApJL in press astro-ph/0210666
- Fukugita, M., Hogan, C. J., & Peebles, P. J. E. 1998, ApJ, 503, 518
- Kashyap, V. & Drake, J. J., 2000, Bull. Astron. Soc. India, 28, 475
- Heckman, T. M. , Norman, C. A., Strickland, D. K. and Sembach, K. R., 2002, ApJ in press (astro-ph/0205556)
- Hellsten, U., Gnedin, N. Y., & Miralda-Escudé, J. 1998, ApJ, 509, 56
- Lockman, F. J. & Savage, B. D. 1995, ApJS, 97, 1
- Ma, C. et al. 1998, AJ, 116, 516
- Mathur, S., Weimberg, D. H. & Chen, X., 2002, proceedings of the conference "IGM/Galaxy Connection- The Distribution of Baryons at $z=0$ ", astro-ph/0210575
- Morrison, R. & McCammon, D. 1983, ApJ, 270, 119
- Nicastro, F. et al. 2001, (astro-ph/0102455)
- Nicastro, F. et al. 2002, ApJ, 573, 157
- Nicastro, F., 2002, private communication
- Penton, S. V., Stocke, J. T., & Shull, J. M. 2000, ApJS, 130, 121
- Rumph, T., Bowyer, S., & Vennes, S. 1994, AJ, 107, 2108
- Sembach, K. R. et al. 2000, ApJ, 538, L31
- Sembay, S., Edelson, R., Markowitz, A., Griffiths, R. G., & Turner, M. J. L. 2002, ApJ, 574, 634
- Shull, J. M., Stocke, J. T., & Penton, S. 1996, AJ, 111, 72

Tripp, T. M., Giroux, M. L., Stocke, J. T., Tumlinson, J., & Oegerle, W. R. 2001, ApJ, 563, 724

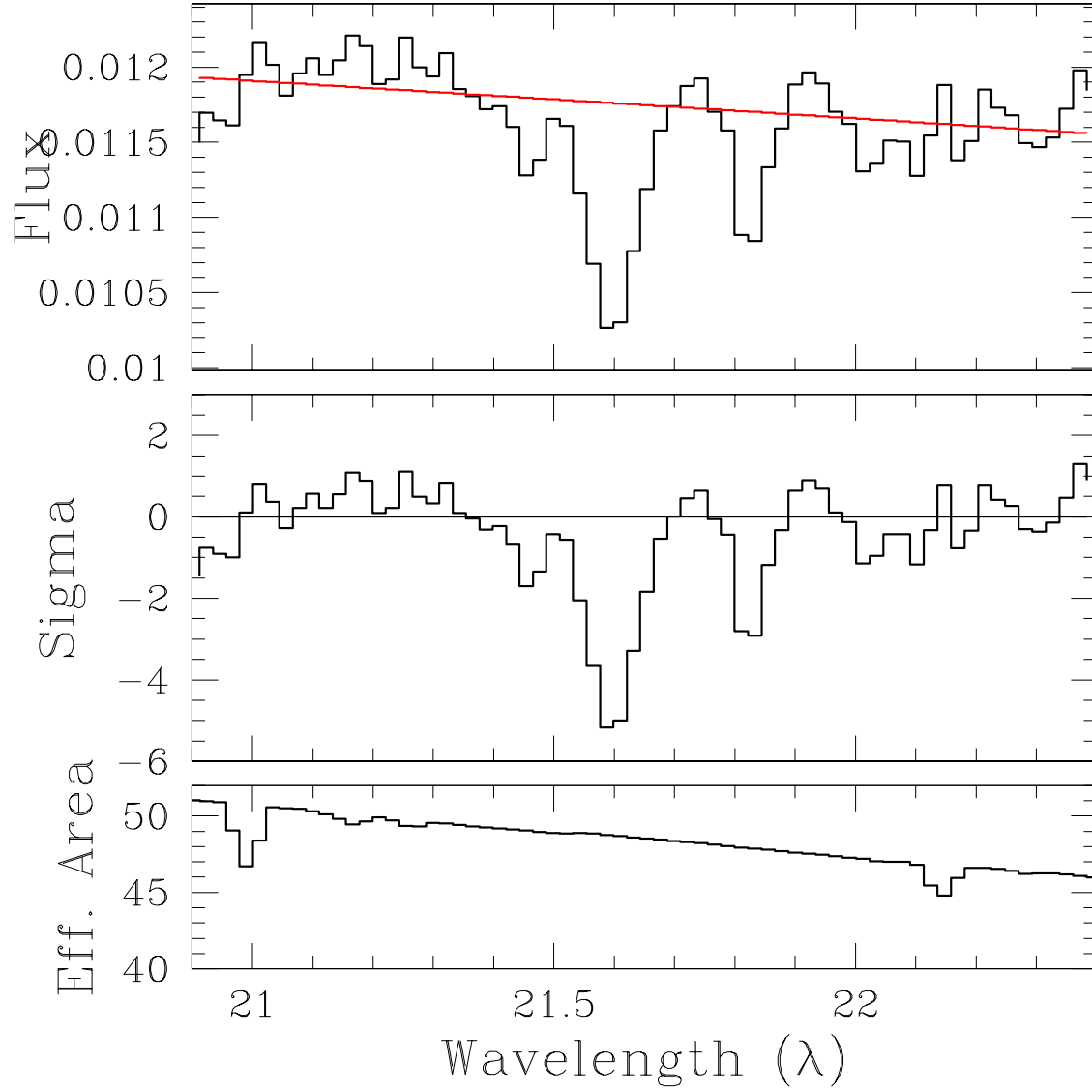


Fig. 1.— Top panel: MRK 421 20.9–22.6 Å combined RGS-1 spectrum and best fit absorbed power law. Middle panel: residuals to the fit and, bottom panel, RGS-1 combined effective area.

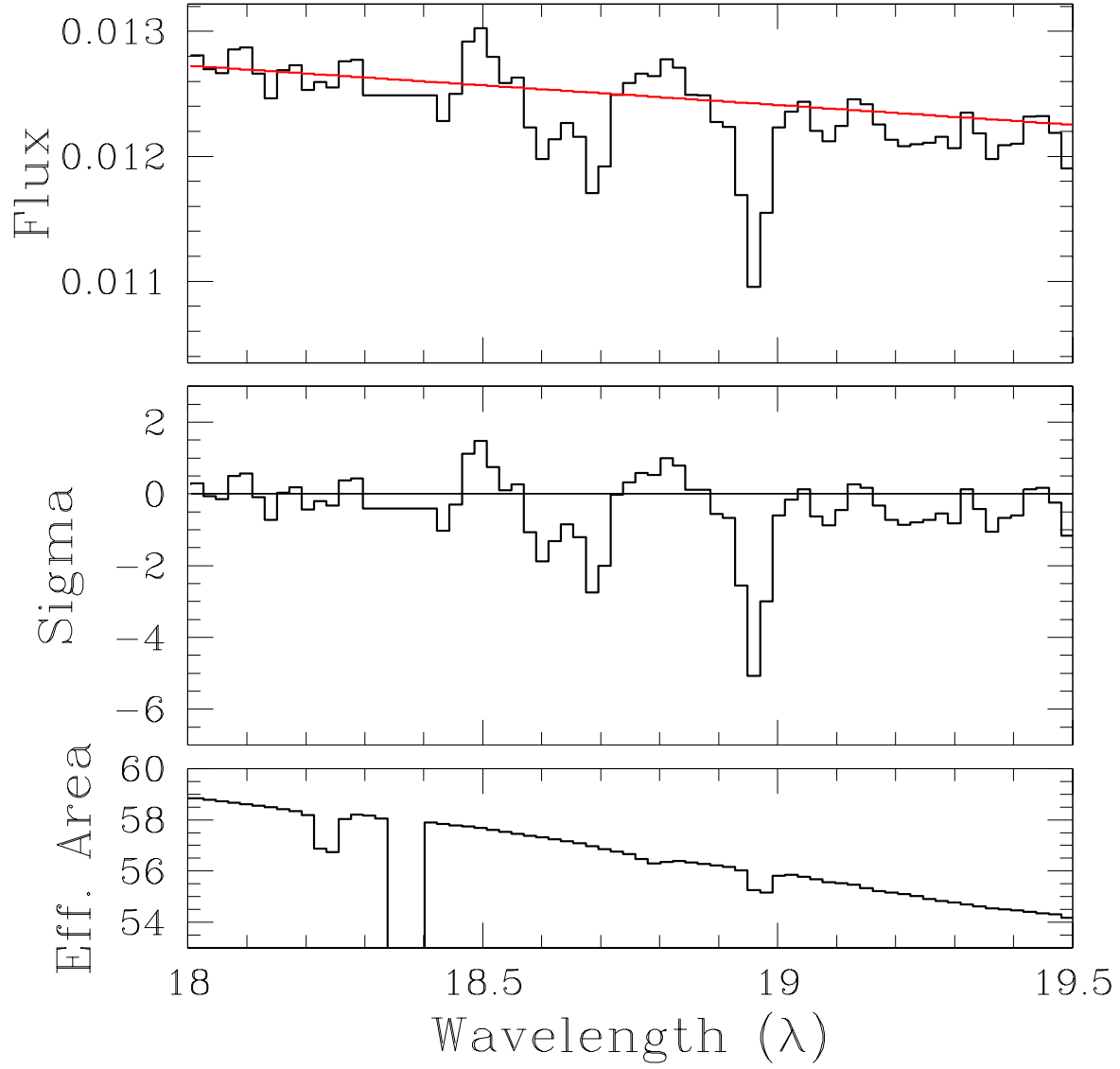


Fig. 2.— Same as Fig. 1 for the 18.0–19.45 Å region.

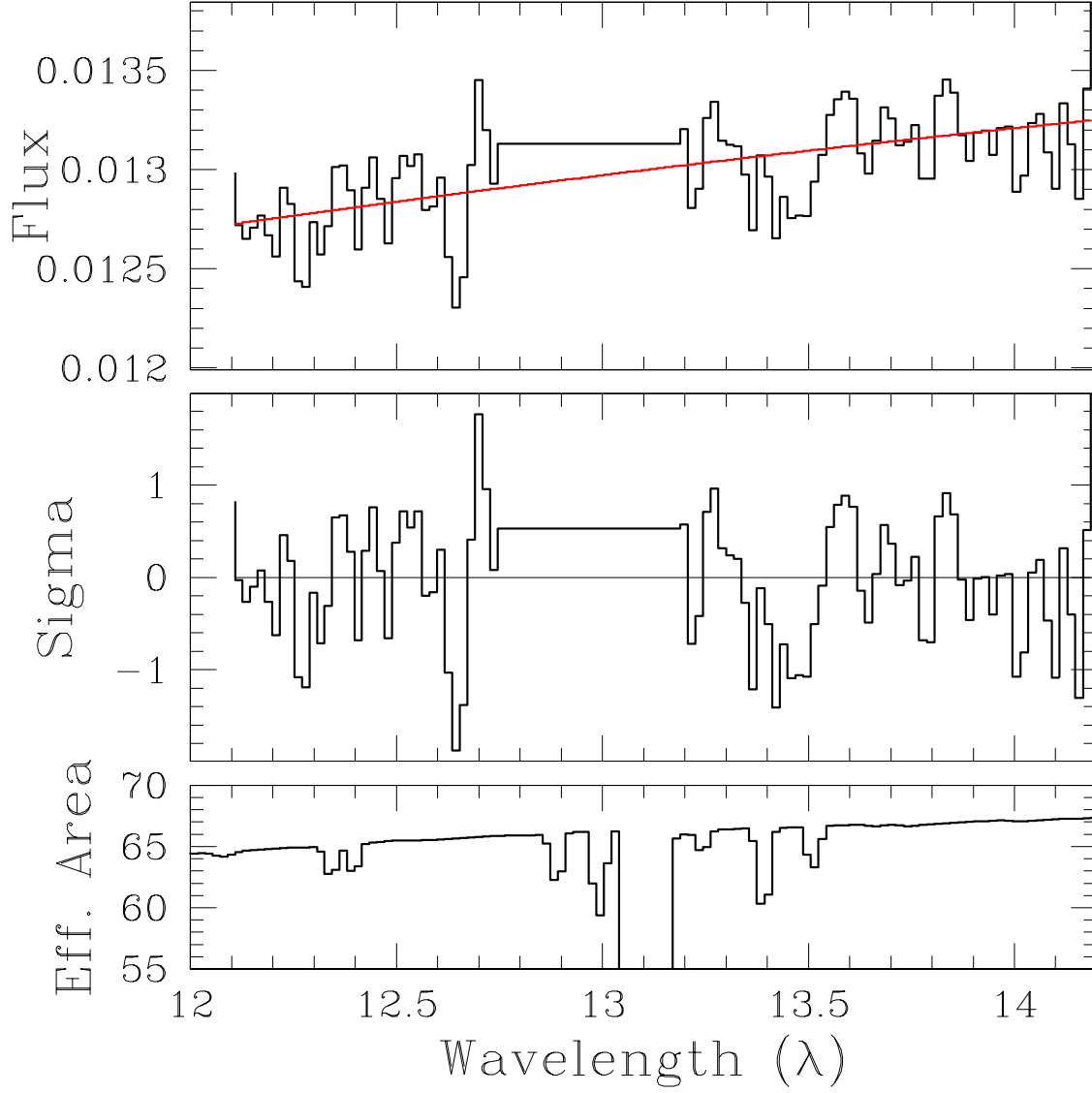


Fig. 3.— Same as Fig. 1 for the RGS-2 vawelength range 12.0–14.2 Å.

Table 1. All the public *XMM-Newton* RGS observations of MRK 421.

Obs. Id.	Obs. Start time ^a	Total Exposure ^b	Net Exposure ^c	Offset	Used observartion? ^d
0099280201	00-11-01	40	34	6.3	YES
0099280301	00-11-13	50	40	5.87	YES
0099280401	00-11-14	43	27	116.69	NO
0099280501	00-11-13	21	15	7.63	YES
0099280601	00-11-15	20	12	117.4	NO
0136540101	01-05-08	39	36	12.95	YES
0136540201	01-05-08	10	0	13.16	NO
0153950601	02-05-04	40	39	123.98	NO
0153950701	02-05-05	20	18	169.43	NO
0153950801	02-05-05	22	21	177.49	NO

^aYY-MM-DD

^bTotal RGS-1 (\sim RGS-2) on time in ks.

^cFor RGS-1 in ks after the high particle background times rejection. RGS-2 net exposure times are similar.

^dFor details see footnote 2 in the text.

Table 2: Best-fitting RGS-1 absorption line parameters and 1σ errors.

Line ID	λ (Å)	cz (km s ⁻¹)	FWHM (10 ⁻² Å)	EW ^a (mÅ)	σ
NeIX ^b	13.441 ± 0.029	-163^{+659}_{-616}	$12.06^{+4.71}_{-11.43}$	$3.52^{+1.70}_{-1.47}$ ($2.89^{+1.30}_{-1.23}$)	2.5
OvII K β	$18.659^{+0.023}_{-0.019}$	486^{+376}_{-299}	$11.22^{+2.80}_{-10.07}$	$5.47^{+10.67}_{-1.63}$ ($4.88^{+1.29}_{-1.37}$)	3.8
OvIII Ly α ^b	18.961 ± 0.008	-98^{+41}_{-39}	$3.27^{+10.01}_{-17.34}$	$5.50^{+5.72}_{-1.09}$ ($7.98^{+1.31}_{-1.33}$)	4.8
OvII K α	21.597 ± 0.008	-75 ± 80	$8.77^{+1.62}_{-1.33}$	$12.67^{+1.59}_{-1.54}$	7.6
OvII K α	$21.822^{+0.027}_{-0.024}$	3062^{+333}_{-375}	$2.77^{+0.83}_{-1.25}$	$3.68^{+4.70}_{-0.70}$	2.8

^aThe values in parenthesis are obtained fixing the FWHM of the line to the value of the zero redshift OvII K α

^bThese lines could possibly be enhanced or modified by the presence of small effective area features (see the bottom panels in Fig. 2 and Fig. 3)